




Article

Tannic Acid-Capped Gold Nanoparticles as a Novel Nanozyme for Colorimetric Determination of Pb²⁺ Ions

Kseniya V. Serebrennikova, Nadezhda S. Komova, Anna N. Berlina , Anatoly V. Zherdev 
and Boris B. Dzantiev * 

A.N. Bach Institute of Biochemistry, Research Center of Biotechnology of the Russian Academy of Sciences, Leninsky Prospect 33, 119071 Moscow, Russia; ksenijasereb@mail.ru (K.V.S.); nad4883@yandex.ru (N.S.K.); anberlina@yandex.ru (A.N.B.); zherdev@inbi.ras.ru (A.V.Z.)

* Correspondence: dzantiev@inbi.ras.ru

Abstract: In this study, tannic acid-modified gold nanoparticles were found to have superior nanozyme activity and catalyze the oxidation reaction of 3,3',5,5'-tetramethylbenzidine in the presence of hydrogen peroxide. Enhancing the catalytic activity of the nanozyme by Pb²⁺ ions caused by selectively binding metal ions by the tannic acid-capped surface of gold nanoparticles makes them an ideal colorimetric probe for Pb²⁺. The parameters of the reaction, including pH, incubation time, and concentration of components, were optimized to reach maximal sensitivity of Pb²⁺ detection. The absorption change is directly proportional to the Pb²⁺ concentration and allows the determination of Pb²⁺ ions within 10 min. The colorimetric sensor is characterized by a wide linear range from 25 to 500 ng×mL^{−1} with a low limit of detection of 11.3 ng×mL^{−1}. The highly sensitive and selective Pb²⁺ detection in tap, drinking, and spring water revealed the feasibility and applicability of the developed colorimetric sensor.

Keywords: colorimetric sensor; gold nanoparticles; tannic acid; nanozyme; catalytic activity; heavy metal detection; lead; water pollution



Citation: Serebrennikova, K.V.; Komova, N.S.; Berlina, A.N.; Zherdev, A.V.; Dzantiev, B.B. Tannic Acid-Capped Gold Nanoparticles as a Novel Nanozyme for Colorimetric Determination of Pb²⁺ Ions.

Chemosensors **2021**, *9*, 332. <https://doi.org/10.3390/chemosensors9120332>

Academic Editor: Gajanan Ghodake

Received: 20 October 2021

Accepted: 22 November 2021

Published: 25 November 2021

Publisher's Note: MDPI stays neutral with regard to jurisdictional claims in published maps and institutional affiliations.



Copyright: © 2021 by the authors. Licensee MDPI, Basel, Switzerland. This article is an open access article distributed under the terms and conditions of the Creative Commons Attribution (CC BY) license (<https://creativecommons.org/licenses/by/4.0/>).

1. Introduction

The widespread use of toxic metals in the manufacture of batteries, pigments, paints, ammunition, toys, and in other applications has led to environmental pollution and public health problems [1]. Pb²⁺ is one of the most dangerous pollutants as its high levels cause serious damage to the nervous system, renal, kidney, and brain. Moreover, prolonged exposure to low metal concentrations can lead to multiple adverse health effects [2]. In accordance with the World Health Organization guidelines, the level of Pb²⁺ in drinking water should not exceed 10 µg·L^{−1} [3]. Common methods for the determination of Pb²⁺ include flame atomic absorption spectroscopy [4], atomic emission spectroscopy [5], X-ray fluorescence [6], inductively coupled plasma mass spectrometry [7], and electrochemical methods [8,9]. However, implementation of these methods requires high-cost complex instrumentation and time-consuming procedures, which complicates on-site monitoring of target analyte.

The alternative approach is colorimetric methods that provide direct and simple detection of Pb²⁺ ions. The possibility to exclude sophisticated instruments staffed by highly trained personnel enables extensive use of colorimetric methods for the detection of Pb²⁺. The most widely applied analytic technique relies on the use of noble metal nanoparticles (most often, silver and gold nanoparticles) as carriers of various receptor molecules that specifically bind target metal ions. In this case, the surface modification of nanoparticles with various chelating ligands [10–13] and oligonucleotides [14–17] provides highly specific detection of Pb²⁺ [18]. In the presence of detectable heavy metal ions, aggregation of nanoparticles occurs, followed by a concentration-dependent color change,

which is observed with the naked eye or recorded photometrically [19,20]. However, obtaining functionalized nanoparticles increases the complexity and cost of the analysis.

Recently, a great interest has been attracted by nanomaterials with enzyme-like catalytic properties, namely, nanozymes due to their ease of preparation, controlled activity, high stability, and low cost [21]. In the presence of metal ions, the catalytic activity of nanozymes may change, which enables the concentration-dependent colorimetric sensing of target ions [22,23]. Various metallic nanoparticles and nanohybrid materials were found to exhibit intrinsic peroxidase-mimicking activity and produce a colored product by catalyzing the oxidation of the enzyme substrate [21]. Thus, Tang et al. described the use of two-dimensional layered tungsten disulfide (WS_2) nanosheets that possess peroxidase-like activity to design colorimetric sensor for Pb^{2+} detection in environmental and biological samples [24]. It was found that Pb^{2+} ions inhibit the catalytic activity of WS_2 nanosheets, the proposed mechanism of which is blocking the electron transfer from the nanosheets to hydrogen peroxide and, as a result, the lack of ($\bullet\text{OH}$) radicals for the oxidation of the enzyme substrate 3,3',5,5'-tetramethylbenzidine (TMB). Among a variety of peroxidase-mimic nanomaterials, gold nanoparticles (AuNPs) are of particular interest because they are easily synthesized and functionalized by various receptor molecules. The ability of metal ions to affect the catalytic activity of AuNPs is used in a number of colorimetric sensors [25,26]. Thus, Lien et al. reported colorimetric analysis of Hg^{2+} and Pb^{2+} ions using peroxidase-mimic activity of AuNPs in the presence of Pt^{4+} and Bi^{3+} ions allowing to detect the target ions in nanomolar concentrations [27]. It should be noted that due to the mechanism of formation of metal-gold alloys, the colorimetric signal could be influenced by other interfering metal ions present in the sample. In this case, the surface modification of AuNPs makes it possible to improve the selectivity of the colorimetric sensor for detection of a target metal ion [28]. Citrate-stabilized gold nanoparticles were earlier proposed for aggregation analysis of different analytes, including heavy metal ions [29,30]. However, the use of unmodified gold nanoparticles for the determination of lead does not allow reaching a sensitivity higher than $18\text{ }\mu\text{M}$ [29]. It is explained by the absence of a specific recognizing molecule on the particle surface. Since the carboxyl groups of organic acids are capable to interact with many metal ions [31], a coating with functional groups is required to selectively recognize specific ions. Earlier, we developed a colorimetric technique for the determination of Pb^{2+} ions using tannic acid as a modifying agent [20]. The developed aggregation analysis made it possible to detect lead ions with a detection limit of 310 ng/mL . Changing sample/reactants volume ratio reduced the detection limit to 60 ng/mL . The use of catechin as an alternative tanning compound demonstrated the presence of a peroxidase-like activity in modified gold nanoparticles for the specific determination of lead in the H_2O_2 -mediated oxidation of Amplex UltraRed [32]. The work of Yoosaf et al. explained the formation of the shell with necessary functional groups available for interaction with Pb^{2+} ions when synthesizing nanoparticles with the use of different tannins as reducing and stabilizing agents [33].

Herein, AuNPs modified by tannic acid (TA) are proposed as a selective sensing probe for nanozyme-based colorimetric detection of Pb^{2+} in water. The implementation of TA as a capping agent showed a peroxidase-like activity of AuNPs for substrate containing H_2O_2 and TMB. The addition of Pb^{2+} ions further stimulated the catalytic activity of the nanoparticles, resulting in a faster formation of a colored product. The Pb^{2+} -promoted nanozyme activity was investigated under different conditions (pH, concentrations of reactants). The practicability and reliability of nanozyme-based colorimetric sensor was validated through the analysis of Pb^{2+} in drinking, spring and tap water. The proposed approach allows for rapid, sensitive, and easy-to-use tool for monitoring of Pb^{2+} levels without sample pre-treatment.

2. Materials and Methods

2.1. Chemicals and Instruments

All of the heavy metal salts were purchased from the Center of Reference Materials and High-Purity Substances, LTD. (Saint-Petersburg, Russia) and used as stock solutions. Chloroauric acid (HAuCl_4), sodium citrate, potassium carbonate, 3, 3', 5, 5'-tetramethylbenzidine (TMB), dimethyl sulfoxide (DMSO) and tannic acid (TA) were obtained from Sigma Aldrich (St. Louis, MO, USA). 33% hydrogen peroxide was supplied by Fluka (St. Louis, MO, USA). All chemicals were of analytical grade. Ultrapure water ($18.5 \text{ M}\Omega \cdot \text{cm}$ at 22°C ; Millipore, Bedford, MA) was applied for the preparation of aqueous solutions. The colorimetric analysis was carried out in 96-well transparent Costar 9018 polystyrene microplates (Costar, Tewksbury, MA, USA).

Absorption spectra of gold nanoparticles were recorded using a UV-2450 spectrophotometer (Shimadzu Kyoto, Japan). The transmission electron microscopy (TEM) images were obtained by JEM CX-100 electron microscope (Jeol, Tokyo, Japan) with an accelerating voltage of 80 kV. The samples were placed onto 300-mesh grids (Pelco International, Redding, CA, USA) coated with formvar film. Subsequent image analysis was performed using Image Tool software (University of Texas Health Science Center, San Antonio, TX, USA).

2.2. Synthesis of TA-Capped AuNPs

The stock solution of TA-capped AuNPs was prepared according to our previous study [31]. Briefly, the solution 1 was prepared by adding 100 μL of 5% HAuCl_4 to 39.5 mL of water. The solution 2 was prepared by mixing 2 mL of 1% sodium citrate, 250 μL of 1% TA, and 250 μL of 0.025 M potassium carbonate in 7.5 mL of ultrapure water. Both solutions were heated to 60°C , followed by pouring solution 2 into solution 1, boiling for 4–5 min and cooling to room temperature. The concentration of prepared TA-capped AuNPs was 10^{-8} M . The solution was stored at $4\text{--}6^\circ \text{C}$ prior to use.

2.3. Comparison of Catalytic Activity of TA-Capped AuNPs in the Absence/Presence of Pb^{2+}

The peroxidase-mimic activity of TA-capped AuNPs was investigated by assessing the ability of nanozyme to oxidize a colorless peroxidase substrate (TMB) into a colored product in the presence of H_2O_2 . The assay was performed at a fixed concentration of TA-capped AuNPs using 500 μM freshly prepared TMB (1% TMB prepared in DMSO) and 500 mM H_2O_2 in sodium citrate buffer (pH 4.0). The kinetic analysis was performed by varying the concentration of H_2O_2 (0.1–0.6 M) at a fixed concentration of TA-capped AuNPs and TMB (500 μM). Similarly, the TMB- H_2O_2 catalytic reaction was carried out by varying the concentration of TMB (0.2–1 mM) with 500 mM H_2O_2 . The reaction was started by adding an appropriate amount of H_2O_2 , and the optical density at 650 nm corresponding to the maximum of TMB oxidation product was recorded using an EnSpire Multi-mode Plate Reader (PerkinElmer, USA). The initial reaction rates were determined from initial linear segment of “ A_{650} -time” curve, reflecting growing concentration of the TMB oxidation product. To calculate the initial reaction rates, the molar absorption coefficient ϵ (650 nm), equal to $39,000 \text{ M}^{-1}\text{cm}^{-1}$ was used. To determine Michaelis-Menten constant (K_m) and maximum reaction velocity (V_{\max}), kinetic dependences were plotted in the Lineweaver-Burk coordinates and the following equation was used:

$$\frac{1}{V_0} = \frac{K_m}{V_{\max}} \times \frac{1}{[S]_0} + \frac{1}{V_{\max}},$$

where V_0 —initial reaction velocity, V_{\max} —maximum reaction velocity, S_0 —initial substrate concentration, K_m —Michaelis-Menten constant.

2.4. Colorimetric Detection of Pb^{2+} in Aqueous Solutions

Briefly, 100 μL of different concentrations of Pb^{2+} solutions were added to 20 μL of TA-capped AuNPs. After incubation for 5 min at room temperature, 50 μL of TMB solution

containing 6% H_2O_2 was added. Immediately, 50 μL of 1M H_2SO_4 was added to stop the reaction. To quantify the concentration of Pb^{2+} the absorbance at 450 nm (A_{450}) was recorded. Each experiment was repeated three times. Dynamic range was determined by plotting A_{450} nm with increasing Pb^{2+} concentration. The limit of detection (LoD) was defined using the equation $3 \times \sigma$, where σ is the standard deviation of the colorimetric signal of the blank sample.

2.5. Specificity of the Analysis

The specificity of the proposed colorimetric sensor was evaluated by testing samples of 13 metal and metalloid ions, namely Hg^{2+} , Zn^{2+} , Cu^{2+} , Co^{2+} , Sr^{2+} , Mn^{2+} , Fe^{3+} , Sn^{4+} , Cr^{3+} , Cd^{2+} , As^{2+} , Sb^{3+} , and Ba^{2+} . 100 μL of the listed ions at a concentration of $100 \text{ ng} \cdot \text{mL}^{-1}$ were added to 15 μL of TA-capped AuNPs. Furthermore, the experiment was carried out as described in Section 2.4.

2.6. Analysis of Real Water Samples

To verify the practical feasibility of the developed sensor, drinking, spring, and tap water samples were analyzed. The container was rinsed with water to be collected at least three times prior to sampling. The samples were purified using a membrane filter with a pore size of $0.22 \mu\text{m}$, after which concentrated HNO_3 was added to preserve the sample and adjust pH to 4.5–5.0. Water samples were stored in a freezer until analysis. A series of spiked water samples, containing Pb^{2+} at concentrations 25, 50, and $100 \text{ ng} \cdot \text{mL}^{-1}$, were prepared by diluting Pb^{2+} stock solution ($0.1 \text{ mg} \cdot \text{mL}^{-1}$ in deionized water). The processing of obtained data was performed using Excel and OriginPro9 (Origin Lab, Northampton, MA, USA).

3. Results

3.1. Characterization of TA-Capped AuNPs

TA-capped AuNPs were prepared by reduction of chloroauric acid by citric and tannic acids, with the latter also providing a stabilizing effect. The as-prepared gold nanoparticles were characterized by wine-red color with an absorption peak at 515 nm (Figure 1a). The morphology of the nanoparticles was observed by TEM (Figure 1b) and revealed monodisperse nanoparticles with the particle size distribution of $6.8 \pm 0.9 \text{ nm}$ (the counted number of particles was 94, Figure 1c).

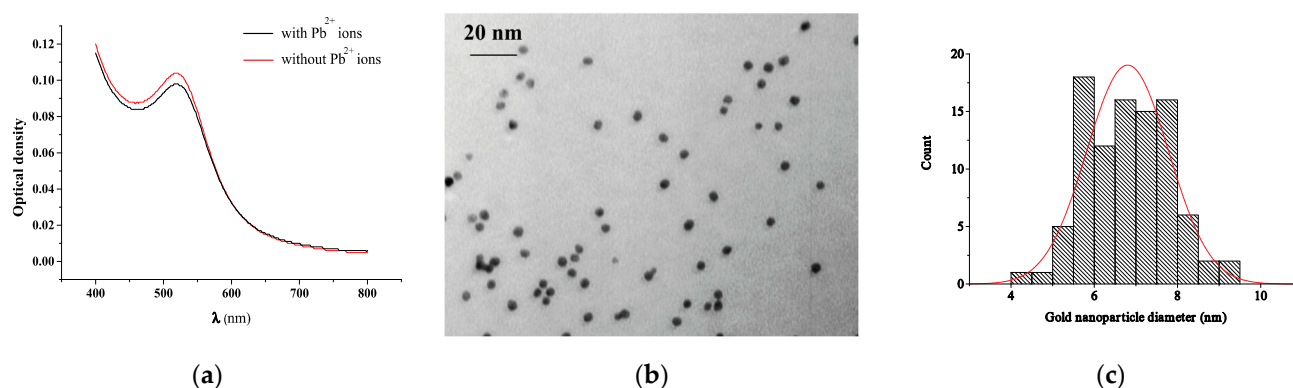


Figure 1. (a) Absorbance spectra of TA-capped AuNPs with (black lines) and without (red lines) Pb^{2+} ions. (b) TEM image and (c) histogram of diameter distribution of the obtained TA-capped AuNPs.

The data on the reproducibility of the synthesis were evaluated in experiments with the determination of the optical density of nanoparticles. Thus, during the synthesis of nanoparticles, the optical density was estimated at 515 nm, which after five repeated syntheses was 0.98, 1.0, 0.98, 0.99, and 0.98, respectively. In addition, the value of the average error of detection was estimated when interacting with lead ions, which was no more than 5.8%.

3.2. Principle of the Nanozyme-Based Colorimetric Pb^{2+} Detection

The principle of proposed colorimetric sensor is illustrated in Figure 2. For Pb^{2+} sensing, TA-capped AuNPs were prepared and applied. Figure 2 clearly demonstrates the mechanism of reaction, absorbance peaks as well as visually observed changes occurred under interaction of nanoparticles with lead ions.

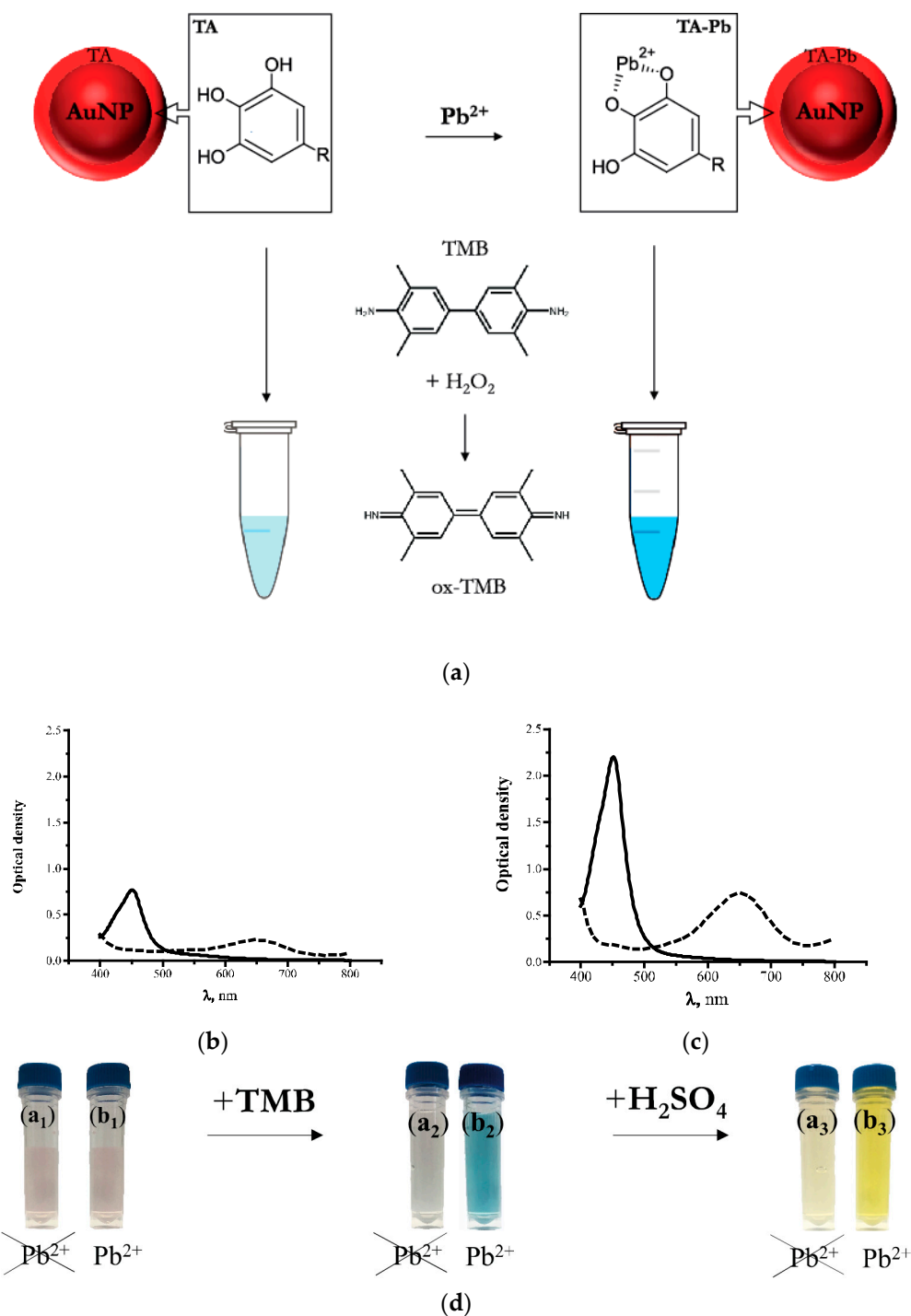


Figure 2. Principle of the TA-capped AuNPs based colorimetric sensor for Pb^{2+} detection. (a) Scheme of catalytic oxidation of TMB in presence of AuNPs. (b) Absorbance spectra of TA-capped AuNPs without and with (c) Pb^{2+} ions after addition of TMB- H_2O_2 (dash lines) and stop reaction (solid lines) respectively. (d) Corresponding photographs of TA-capped AuNPs samples before/after catalytic reaction in the presence/absence Pb^{2+} ions.

The scheme of the reactants' interaction and catalytic oxidation of TMB by TA-capped AuNPs is presented on Figure 2a. In the absence of Pb^{2+} ions AuNPs had weak catalytic activity toward TMB oxidation. Due to this, low absorbance at 650 nm was observed, and visually confirmed by the weak color development (Figure 2b). In the presence of lead, tannic acid residues chelated Pb^{2+} ions to form the complexes indicated at Figure 2a. This interaction promoted the catalytic activity of the AuNPs as nanozymes and resulted in increasing of absorbance peak at 650 nm related to oxidated product of TMB transformation (Figure 3c), the color of solution became bright blue. After adding the sulfuric acid stop solution, the blue color turned to yellow and thus absorbance peak at 450 nm increased (Figure 3d). The addition of a TMB solution to a solution of lead ions and tannic acid did not lead to any catalytic activity in the absence of AuNPs.

It was previously shown that, in addition to the reducing properties of tannic compounds, they form complexes with metal ions [34–36]. The proposed mechanism of the analytical use of such tannic acid-containing nanoparticles is as follows. AuNPs synthesized with TA as a reducing and stabilizing agent have carbonyl groups on their surface and able to hydrolysis of phenolic compounds. They, in turn, specifically bind to Pb^{2+} ions, providing the formation of bridges that unite several nearby modified nanoparticles into clusters. This arrangement and the presence of free electron orbitals of Pb^{2+} cations provide a free transition of an electron participating in the oxidation reaction of the substrate (TMB). The proposed principle of Pb^{2+} colorimetric detection corresponds to the previously described “turn-on” mechanism based on the enhancement of the catalytic activity of noble metal nanoparticles in the presence of metal ions [22].

The mechanism of oxidation of TMB catalyzed by AuNPs as a peroxidase-like nanozyme has been considered in earlier [28,37]. The catalytic process is similar to the Fenton reaction [38] and includes the following stages: (1) the formation of a hydroxyl radical (OH^\cdot) from hydrogen peroxide in the presence of nanozyme, (2) the oxidation of TMB by the hydroxyl radical with the formation of the blue product TMB^+ . The high affinity of gold nanoparticles for TMB accelerates the excited electron transfer, which complicates the recombination of electron-hole pairs and, in turn, promotes the formation of OH^\cdot . Thus, the peroxidase-like activity is increased. In addition, the presence of lead ions stimulates the formation of hydroxyl radicals [39].

3.3. Optimization of the Experimental Conditions for Colorimetric Pb^{2+} Detection

As shown in Figure 3a, the reaction of TMB oxidation by H_2O_2 catalyzed by TA-capped AuNPs reaches a plateau after 120 s. This incubation time was used as optimal in further experiments. To select the optimal pH, the catalytic activity of Pb^{2+} -promoted TA-capped AuNPs was studied in a wide pH range from 3.5 to 7.5. As follows from Figure 3b, the highest signal after adding the stopping solution (A_{450}) is recorded in the pH range 4.5–5. Furthermore, the ratios of the components in the colorimetric analysis were optimized by varying concentrations of TA-capped AuNPs, TMB, and H_2O_2 . Figure 3c,d shows that the highest colorimetric signal was observed when 11.8×10^{-10} M TA-capped AuNPs and 0.5 mM TMB were applied. The peroxide-like activity of nanozymes also depends on the concentration of H_2O_2 , since the latter forms hydroxyl radicals that oxidize TMB [40]. In this regard, the influence of the concentration of H_2O_2 on the catalytic activity of Pb^{2+} -promoted TA-capped AuNPs was investigated (Figure 3e). The growth of the H_2O_2 concentration up to 0.53M gives rise to the signal enhancement.

3.4. Colorimetric Technique for Determining the Catalytic Activity of TA-Capped AuNPs

The peroxidase-mimic activity of bare TA-capped AuNPs was investigated using TMB. TMB is a common peroxidase substrate that is oxidized in the presence of H_2O_2 forming a blue product. The mixture of TMB with H_2O_2 is initially colorless; however, when TA-capped AuNPs are added, the mixture turns blue, which indicates the peroxidase-like activity. Nevertheless, the addition of Pb^{2+} to the mixture increases the catalytic activity and the solution instantly acquires a deep blue color (see Figure 2d).

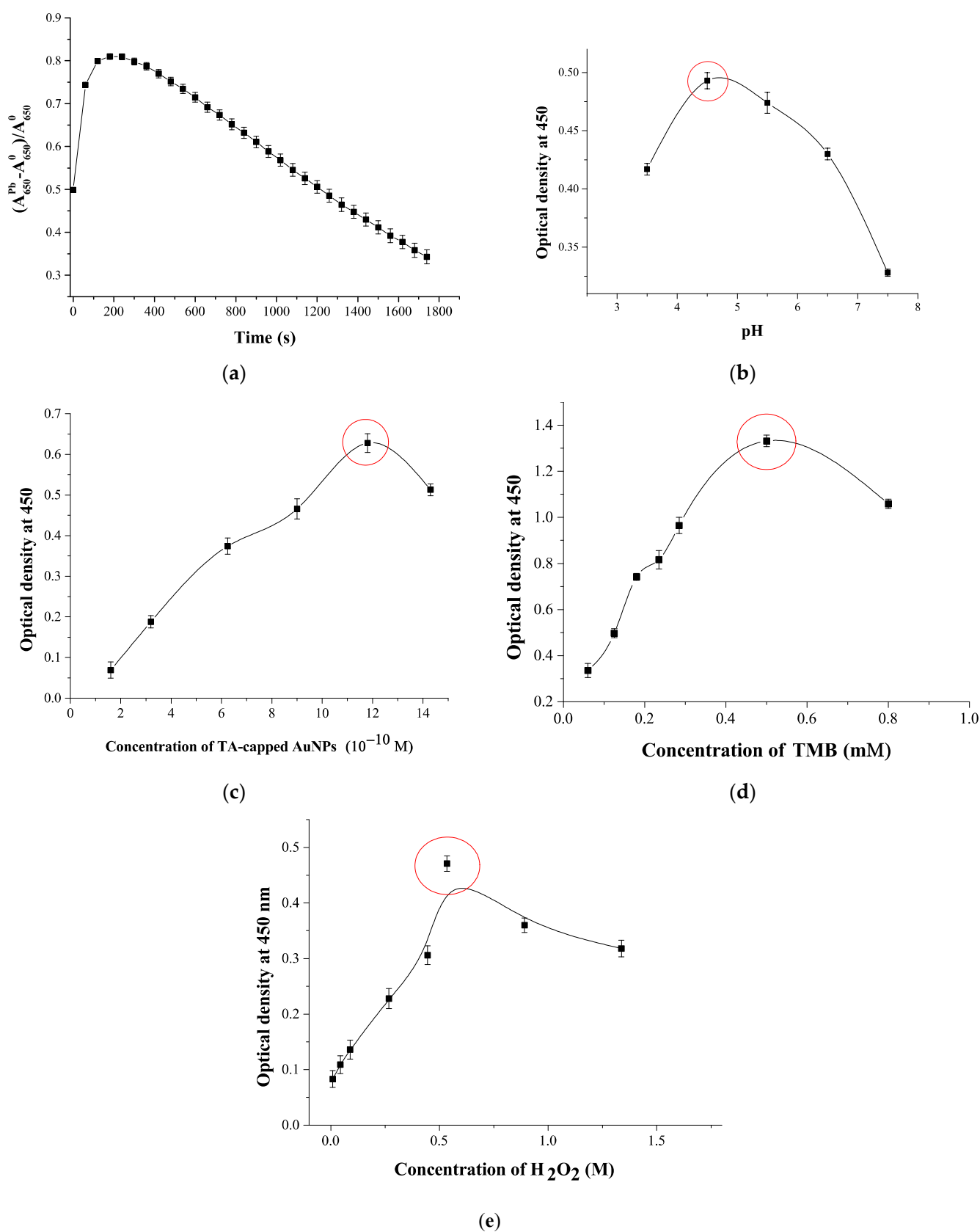


Figure 3. Optimization of the analysis conditions: (a) Time dependence of the colorimetric response in the presence of Pb^{2+} relative to the background signal; (b) pH effect to analytical signal; (c) Concentration of TA-capped AuNPs; (d) Concentration of TMB; (e) Concentration of H_2O_2 . Experimental conditions: 11.8×10^{-10} M TA-capped AuNPs, 0.5 mM TMB, 0.5 M H_2O_2 , $100 \text{ ng} \cdot \text{mL}^{-1}$ Pb^{2+} , pH 4.5. ($N = 3$).

The Pb^{2+} -promoted catalytic activity was investigated comparing the nanoparticles with and without Pb^{2+} and plotting the time dependence of absorbance at 650 nm (stop solution was not added in these studies). As can be seen from the Figure 4, the presence of Pb^{2+} leads to a sharp increase of absorbance. A linear segment of the curve up to 120 s was used to calculate the initial velocity. Thus, the highest rate ($3 \times 10^{-3} \text{ s}^{-1}$) was observed for the nanozyme in the presence of Pb^{2+} , being three times the value of $1 \times 10^{-3} \text{ s}^{-1}$, observed in the absence of Pb^{2+} . The estimated data confirm Pb^{2+} -promoted catalytic activity of TA-capped AuNPs, which can be applied for detection of Pb^{2+} ions.

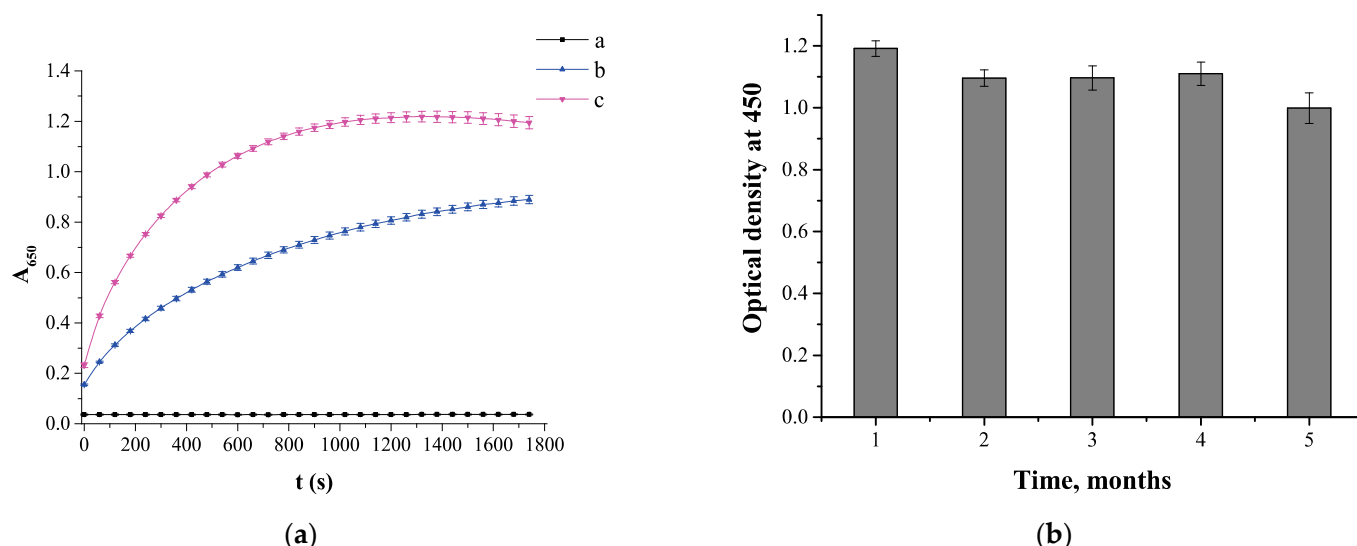


Figure 4. (a) Peroxidase-like activity of TA-capped AuNPs: a—substrate mixture, 0.5 M H_2O_2 + 0.5 mM TMB; b— 11.8×10^{-10} M TA-capped AuNPs + 0.5M H_2O_2 + 0.5 mM TMB; c— 11.8×10^{-10} M TA-capped AuNPs + $100 \text{ ng} \times \text{mL}^{-1}$ Pb^{2+} + 0.5 M H_2O_2 + 0.5 mM TMB. ($N = 3$). (b) Pb^{2+} -promoted catalytic activity of TA-capped AuNPs during long-term storage.

Furthermore, the stability of TA-capped AuNPs was evaluated. The TA-capped AuNPs were stored at 4°C and Pb^{2+} -promoted catalytic activity of the nanozyme was measured every month to investigate long-term stability. As shown in Figure 4b, the nanozyme displays stable high catalytic activity for 4 months, and after this period, it decreases slightly.

To investigate the catalytic properties of the TA-capped AuNPs the kinetic parameters were defined using by varying the concentration of both TMB and H_2O_2 and data processing by the Michaelis-Menten model as described in [41]. The Michaelis-Menten constants (K_m) and maximum initial reaction rates (v_{max}) were calculated by fitting the Lineweaver-Burk plots (Figure 5b,d). As shown in Table 1, the TA-capped AuNPs exhibited a lower K_m value when using TMB as a substrate compared to horseradish peroxidase (HRP) (0.2 mM versus 0.43 mM) indicating the stronger affinity of this nanozyme toward substrate. Pb^{2+} ions enhanced the catalytic activity of TA-capped AuNPs, which is reflected in a decrease of the K_m to 0.09 mM. In contrast, the K_m determination for H_2O_2 as a substrate revealed much higher values than that of HRP (190 mM versus 3.7 mM, see Table 1), highlighting the need for H_2O_2 concentrations to ensure maximum catalytic activity of the nanozyme. As previously shown [42], strong affinity of HRP for H_2O_2 is due to the presence of amino acids in the active centre of the natural enzyme. To sum up, these results demonstrated Pb^{2+} -promoted nanozyme activity, and TA-capped AuNP is an appropriate sensing probe for Pb^{2+} detection.

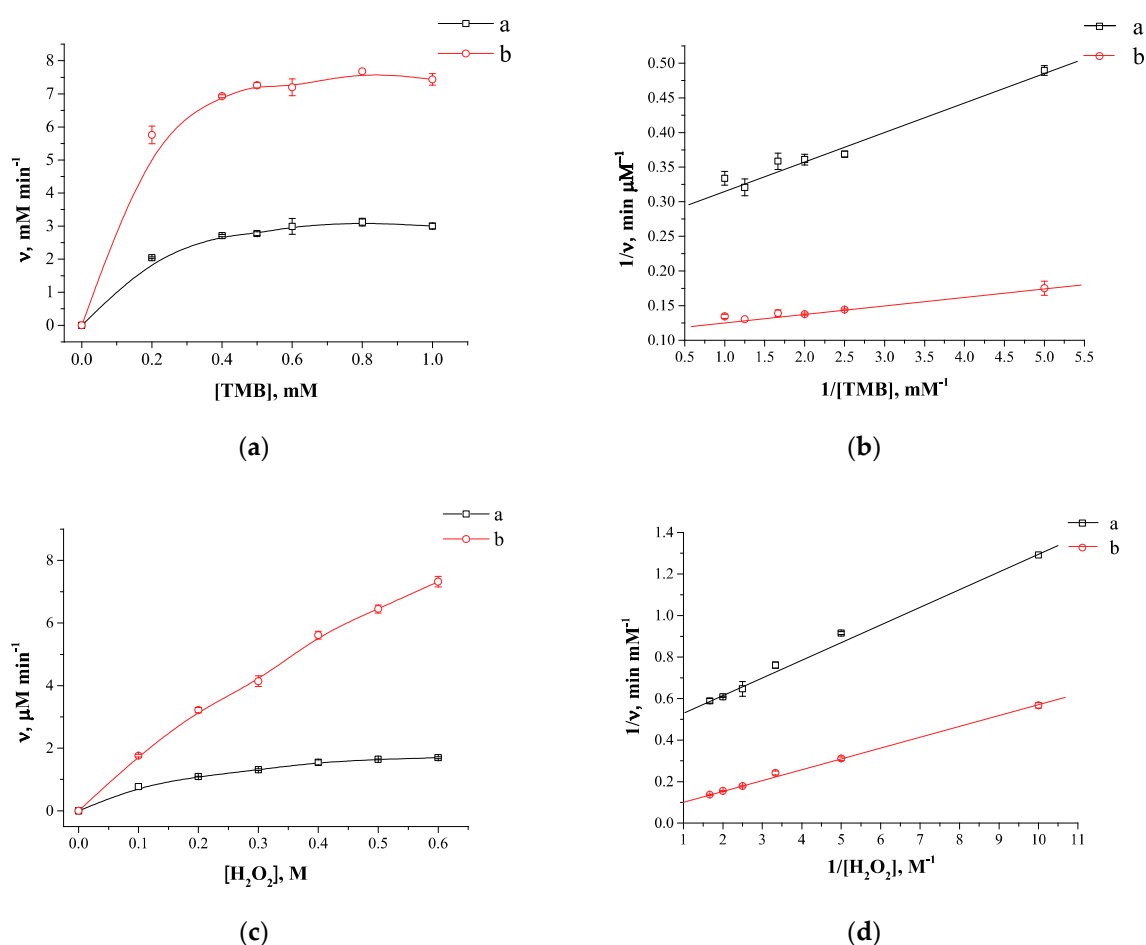


Figure 5. Kinetic dependences of Michaelis-Menten and their linear transformations in double reciprocal plots (Lineweaver-Burk plots) for TA-capped AuNPs with (a, black lines) and without (b, red lines) Pb^{2+} ions varying the concentration of TMB from 0.2 to 1 mM with a fixed concentration of H_2O_2 at 0.5 M (a,b) and varying the concentration of H_2O_2 from 0.1 to 0.6 M with a fixed TMB at 0.5 mM (c,d). ($N = 3$). The values of deviations from the mean at the points for figures a-e are, respectively, 0.6–4.6%, 0.6–5.8%, 0.5–5.5%, 0.5–4.1%.

Table 1. Comparison of kinetic parameters (K_m and v_{\max}) of the oxidation reaction catalyzed by HRP and the proposed colorimetric probe.

Sensing probe	[E] (M)	Substrate	K_m (mM)	v_{\max} (M s^{-1})
TA-capped AuNPs	11.8×10^{-10}	TMB	0.2	6.7×10^{-8}
		H_2O_2	190	3.8×10^{-8}
Pb^{2+} -TA-capped AuNPs	11.8×10^{-10}	TMB	0.09	1.4×10^{-7}
		H_2O_2	100	3.3×10^{-7}
HRP [43]	6.2×10^{-11}	TMB	0.43	10×10^{-8}
		H_2O_2	3.7	8.7×10^{-8}

3.5. Quantitative Pb^{2+} Detection Using Colorimetric Sensor

According to the TA-capped AuNPs-based colorimetric sensor design format, the amount of Pb^{2+} ions determine the peroxide-mimicking activity of the sensing probe. Consequently, the sensing responses of Pb^{2+} ions with different concentrations were investigated under optimal conditions. To assess the sensitivity and dynamic linear range of the developed sensor, concentrations of Pb^{2+} from 1 to 1000 $\text{ng} \times \text{mL}^{-1}$ were tested, and A_{450} was measured. As shown in Figure 6, with an increase in the Pb^{2+} concentration, A_{450} increases, accompanied by a color change from light blue to dark blue. The dynamic

linear range for Pb^{2+} detection is $25\text{--}500\text{ ng}\times\text{mL}^{-1}$ with the linear regression equation of $y = 0.406 - 0.03x$ and correlation coefficient (R^2) of 0.994 (Figure 6b). The detection limit is calculated to be $11.3\text{ ng}\times\text{mL}^{-1}$ using the signal-to-noise ratio ($S/N = 3$), which is roughly in line with WHO drinking water guideline of $10\text{ ng}\times\text{mL}^{-1}$. The linearity and Pb^{2+} detection limit of the developed sensor was mapped to previously reported colorimetric sensors and summarized in Table 2. The proposed colorimetric sensor allows the detection of Pb^{2+} ions in the nanogram range without additional sample pretreatment and demonstrates comparable or superior performance compared to other colorimetric analyses reported in the literature [13,41,43,44].

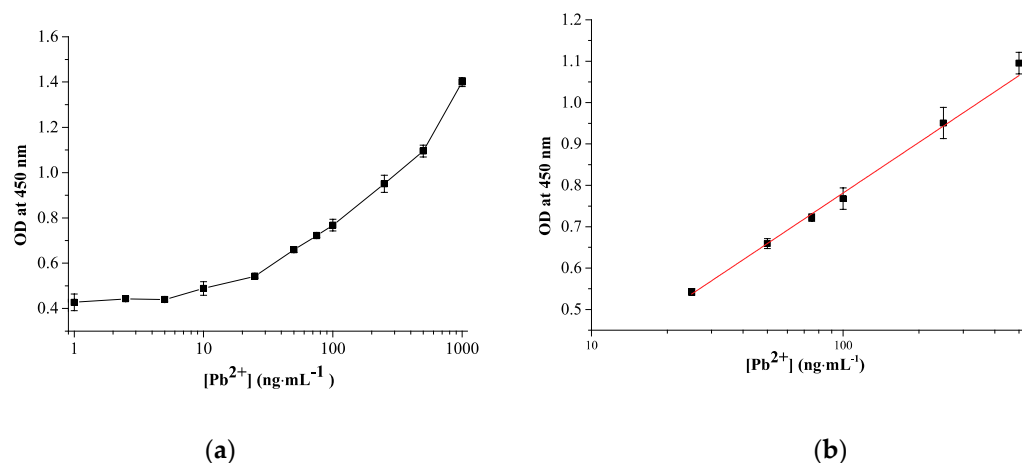


Figure 6. Calibration curve for detection of Pb^{2+} ions using TA-capped AuNPs (a) and its linear range (b) ($N = 3$).

Table 2. Comparison of the developed analysis for Pb^{2+} with previously reported colorimetric methods.

Sensing Material	Sensing Mechanism	LOD ($\text{ng}\times\text{mL}^{-1}$)	Linear Range ($\text{ng}\times\text{mL}^{-1}$)	Analysis Time (min)	Ref
Rapid assays					
TA-capped AuNPs	Pb^{2+} -promoted nanozyme activity of TA-capped AuNPs	11.3	25–500	10	This work
1-(2-mercaptoethyl)-1,3,5-triazinane-2,4,6-trione functionalized silver nanoparticles (MTT-AgNPs)	aggregation of the MTT–AgNPs in the presence of Pb^{2+} ions	19.8	103–600	3	[44]
N-decanoyltromethamine(NDTM)-capped AuNPs	Pb^{2+} -induced aggregation of NDTM-AuNPs	72.4	0–6200	<1	[13]
Oligonucleotide functionalized AuNPs	Change in guanine-rich ssDNA conformation into a rigid G-quartet structure in the presence of Pb^{2+} and NaCl-induced aggregation of unmodified AuNPs	1035	20.7–2070	5	[45]
AuNPs	Aggregation of the as-synthesized AuNPs in the presence of Pb^{2+}	3730	$0\text{--}20.7 \times 10^3$	<5	[29]
Valine-capped AuNPs	Pb^{2+} -induced aggregation of valine-capped AuNPs	6300	$0\text{--}289 \times 10^3$	5	[46]

Table 2. Cont.

Sensing Material	Sensing Mechanism	LOD ($\text{ng} \times \text{mL}^{-1}$)	Linear Range ($\text{ng} \times \text{mL}^{-1}$)	Analysis Time (min)	Ref
Time consuming assays					
Catechin synthesized AuNPs	Pb ²⁺ -promoted nanozyme activity of catechin modified AuNPs in the H ₂ O ₂ -mediated oxidation of Amplex UltraRed	0.3	2–207	60	[32]
Gold core-platinum shell nanohybrids (Au@PtNPs)	Pb ²⁺ -S ₂ O ₃ ²⁻ ions-inhibited nanozyme activity of Au@PtNP	0.6	4–166	40	[47]
Sodium thiosulfate and hexadecyl trimethyl ammonium bromide (CTAB) modified AuNPs	leaching of CTAB-capped Au NPs induced by Na ₂ S ₂ O ₃ and Pb ²⁺	8.3	207–1200	30	[48]

3.6. Selectivity

To confirm the specificity of the nanozyme-based colorimetric sensor, along with Pb²⁺, the contribution of other metals to the colorimetric response was studied. The concentration of all tested ions was 100 $\text{ng} \times \text{mL}^{-1}$. As shown in Figure 7, the reaction solution containing Pb²⁺ showed bright yellow while competing metal ions were almost colorless. All interfering metal ions demonstrated almost negligible changes in A₄₅₀ after stopping the oxidation reaction (Figure 7). Thus, the results demonstrate excellent selectivity of TA-capped AuNPs toward Pb²⁺ ions among all interfering metal ions. The results obtained in this study are in accordance with previously reported data on strong adsorption capacity of tannin compounds toward Pb²⁺ ions in comparison to other metal [49,50].

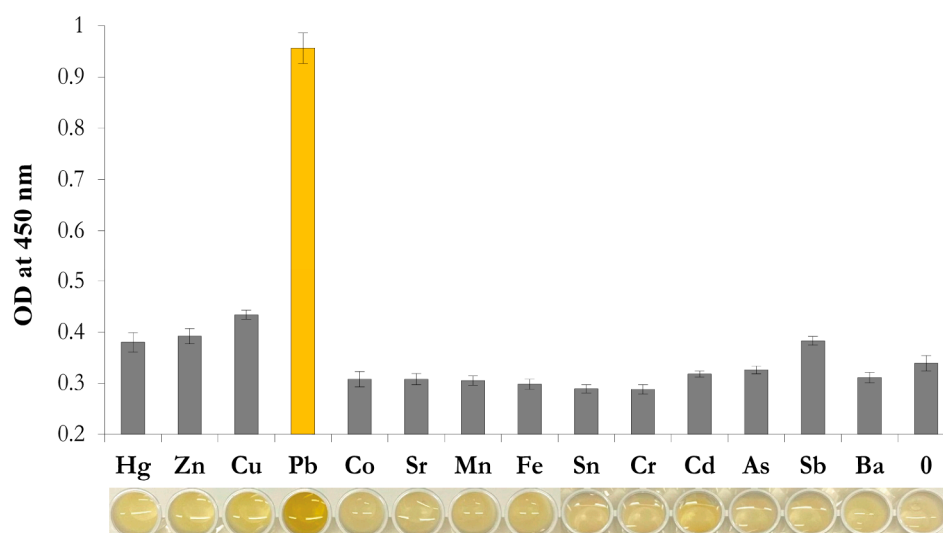


Figure 7. Selectivity of the TA-capped AuNPs toward various metal ions with a concentration of 100 $\text{ng} \times \text{mL}^{-1}$. ($N = 3$). Insert: images of reaction media after testing the listed metal ions.

3.7. Evaluation of Nanozyme-Based Colorimetric Sensor

To evaluate the practicability of the developed approach, the detection of Pb²⁺ was performed in drinking, spring, and tap water. It was found that there were no Pb²⁺ ions in spring, bottled drinking and tap water samples, therefore known concentrations of Pb²⁺ (25, 50, and 100 $\text{ng} \times \text{mL}^{-1}$) were added to them. Table 3 shows the results of Pb²⁺ detection in spiked water samples. The obtained recoveries were from 106.6% to 133.4% with relative

standard deviation less than 8%. These results indicate good precision and accuracy of the Pb^{2+} detection in real water samples.

Table 3. Colorimetric detection of Pb^{2+} in spiked water samples.

Sample	Added ($\text{ng} \times \text{mL}^{-1}$)	Found ($\text{ng} \times \text{mL}^{-1}$)	Recovery (%)	RSD (%; n = 3)
Drinking water	25	33.3	133.4	2.8
	50	54.5	108.9	3.2
	100	128.2	128.2	5.6
Tap water	25	27.7	110.9	2.9
	50	56.5	112.9	7.7
	100	106.6	106.6	3.8
Spring water	25	29.7	118.7	1.9
	50	56.8	113.6	2.9
	100	106.8	106.8	6.3

4. Conclusions

To sum up, a novel colorimetric sensor for Pb^{2+} detection in water was developed based on peroxidase-like properties of small-sized TA-capped AuNPs. It was found that TA-capped AuNPs catalyze the oxidation of TMB by H_2O_2 under slightly acidic environment, thus providing a simple colorimetric detection of Pb^{2+} ions. The detection limit of Pb^{2+} ions was $11.3 \text{ ng} \times \text{mL}^{-1}$, which is close to the value established by the WHO guidelines of drinking water quality. The developed sensor was successfully applied to determine Pb^{2+} in real water samples from different sources with good recovery and RSD. Compared to conventional methods for the determination of Pb^{2+} in water, the proposed sensor has a number of tangible advantages, such as: (1) simplicity of the nanozyme preparation without an additional stage of gold nanoparticle modification; (2) excellent analytical performance for Pb^{2+} detection among other interfering metal ions; (3) analysis time takes 10 min. Taken together, these benefits enable to consider the developed colorimetric sensor as one of the approaches for the determination of Pb^{2+} ions in aqueous media, which can be further extended for practical use.

Author Contributions: Conceptualization, K.V.S. and A.N.B.; methodology, N.S.K. and A.N.B.; software, N.S.K.; validation, N.S.K.; formal analysis, K.V.S. and N.S.K.; investigation, K.V.S. and N.S.K.; resources, A.V.Z.; data curation, A.V.Z.; writing—original draft preparation, K.V.S. and A.N.B.; writing—review and editing, K.V.S., A.V.Z. and B.B.D.; visualization, A.V.Z.; supervision, B.B.D.; project administration, B.B.D.; funding acquisition, A.N.B. and B.B.D. All authors have read and agreed to the published version of the manuscript.

Funding: This work was financially supported by the Russian Science Foundation (project # 19-44-02020, assay development) and the Ministry of Science and Higher Education of the Russian Federation (study of assay selectivity).

Institutional Review Board Statement: Not applicable.

Informed Consent Statement: Not applicable.

Data Availability Statement: Not applicable.

Conflicts of Interest: The authors declare no conflict of interest.

References

1. Wani, A.L.; Ara, A.; Usmani, J.A. Lead toxicity: A review. *Interdiscip. Toxicol.* **2015**, *8*, 55–64. [[CrossRef](#)] [[PubMed](#)]
2. Ahamed, M.; Siddiqui, M. Low level lead exposure and oxidative stress: Current opinions. *Clin. Chim. Acta* **2007**, *383*, 57–64. [[CrossRef](#)]
3. WHO. *Guidelines for Drinking-Water Quality*, 4th ed.; WHO: Geneva, Switzerland, 2011.

4. Daşbaşı, T.; Saçmacı, Ş.; Ülgen, A.; Kartal, Ş. A solid phase extraction procedure for the determination of Cd(II) and Pb(II) ions in food and water samples by flame atomic absorption spectrometry. *Food Chem.* **2015**, *174*, 591–596. [\[CrossRef\]](#)
5. Sabarudin, A.; Lenghor, N.; Liping, Y.; Furusho, Y.; Motomizu, S. Automated Online Preconcentration System for the Determination of Trace Amounts of Lead Using Pb-Selective Resin and Inductively Coupled Plasma–Atomic Emission Spectrometry. *Spectrosc. Lett.* **2006**, *39*, 669–682. [\[CrossRef\]](#)
6. Kamilari, E.; Farsalinos, K.; Poulas, K.; Kontoyannis, C.G.; Orkoula, M.G. Detection and quantitative determination of heavy metals in electronic cigarette refill liquids using Total Reflection X-ray Fluorescence Spectrometry. *Food Chem. Toxicol.* **2018**, *116*, 233–237. [\[CrossRef\]](#) [\[PubMed\]](#)
7. Mao, J.; Liu, X.-q.; Chen, B.; Luo, F.; Wu, X.; Jiang, D.; Luo, Z. Determination of heavy metals in soil by inductively coupled plasma mass spectrometry (ICP-MS) with internal standard method. *Electron Sci Technol Appl.* **2017**, *4*, 23–31. [\[CrossRef\]](#)
8. Xu, T.; Dai, H.; Jin, Y. Electrochemical sensing of lead(II) by differential pulse voltammetry using conductive polypyrrole nanoparticles. *Microchim. Acta* **2019**, *187*, 23. [\[CrossRef\]](#) [\[PubMed\]](#)
9. Yadav, R.; Berlina, A.N.; Zherdev, A.V.; Gaur, M.S.; Dzantiev, B.B. Rapid and selective electrochemical detection of pb2+ ions using aptamer-conjugated alloy nanoparticles. *SN Appl. Sci.* **2020**, *2*, 1–11. [\[CrossRef\]](#)
10. Chai, F.; Wang, C.; Wang, T.; Li, L.; Su, Z. Colorimetric Detection of Pb2+ Using Glutathione Functionalized Gold Nanoparticles. *ACS Appl. Mater. Interfaces* **2010**, *2*, 1466–1470. [\[CrossRef\]](#)
11. Qi, L.; Shang, Y.; Wu, F. Colorimetric detection of lead (II) based on silver nanoparticles capped with iminodiacetic acid. *Microchim. Acta* **2012**, *178*, 221–227. [\[CrossRef\]](#)
12. Ratnarathorn, N.; Chailapakul, O.; Dungchai, W. Highly sensitive colorimetric detection of lead using maleic acid functionalized gold nanoparticles. *Talanta* **2015**, *132*, 613–618. [\[CrossRef\]](#)
13. Sengan, M.; Kamlekar, R.K.; Veerappan, A. Highly selective rapid colorimetric sensing of Pb2+ ion in water samples and paint based on metal induced aggregation of N-decanoyltromethamine capped gold nanoparticles. *Spectrochim. Acta Part A Mol. Biomol. Spectrosc.* **2020**, *239*, 118485. [\[CrossRef\]](#)
14. Berlina, A.N.; Zherdev, A.V.; Pridvorova, S.M.; Gaur, M.; Dzantiev, B.B. Rapid Visual Detection of Lead and Mercury via Enhanced Crosslinking Aggregation of Aptamer-Labeled Gold Nanoparticles. *J. Nanosci. Nanotechnol.* **2019**, *19*, 5489–5495. [\[CrossRef\]](#) [\[PubMed\]](#)
15. Xu, H.; Liu, B.; Chen, Y. A colorimetric method for the determination of lead(II) ions using gold nanoparticles and a guanine-rich oligonucleotide. *Microchim. Acta* **2012**, *177*, 89–94. [\[CrossRef\]](#)
16. Wang, F.; Dai, J.; Shi, H.; Luo, X.; Xiao, L.; Zhou, C.; Guo, Y.; Xiao, D. A rapid and colorimetric biosensor based on GR-5 DNAzyme and self-replicating catalyzed hairpin assembly for lead detection. *Anal. Methods* **2020**, *12*, 2215–2220. [\[CrossRef\]](#)
17. Wang, G.; Chu, L.T.; Hartanto, H.; Utomo, W.B.; Pravasta, R.A.; Chen, T.-H. Microfluidic Particle Dam for Visual and Quantitative Detection of Lead Ions. *ACS Sensors* **2019**, *5*, 19–23. [\[CrossRef\]](#) [\[PubMed\]](#)
18. Liu, D.; Wang, Z.; Jiang, X. Gold nanoparticles for the colorimetric and fluorescent detection of ions and small organic molecules. *Nanoscale* **2011**, *3*, 1421–1433. [\[CrossRef\]](#)
19. Komova, N.S.; Serebrennikova, K.V.; Berlina, A.N.; Pridvorova, S.M.; Zherdev, A.V.; Dzantiev, B.B. Mercaptosuccinic-Acid-Functionalized Gold Nanoparticles for Highly Sensitive Colorimetric Sensing of Fe(III) Ions. *Chemosensors* **2021**, *9*, 290. [\[CrossRef\]](#)
20. Berlina, A.; Sharma, A.K.; Zherdev, A.V.; Gaur, M.S.; Dzantiev, B.B. Colorimetric Determination of Lead Using Gold Nanoparticles. *Anal. Lett.* **2014**, *48*, 766–782. [\[CrossRef\]](#)
21. Wong, E.L.S.; Vuong, K.Q.; Chow, E. Nanozymes for Environmental Pollutant Monitoring and Remediation. *Sensors* **2021**, *21*, 408. [\[CrossRef\]](#)
22. BineshUnnikrishnana, C.-W.; Chu, H.-W.; Huang, C.-C. A review on metal nanozyme-based sensing of heavy metal ions: Challenges and future perspectives. *J. Hazard. Mater.* **2021**, *401*, 123397. [\[CrossRef\]](#)
23. Yan, Z.; Yuan, H.; Zhao, Q.; Xing, L.; Zheng, X.; Wang, W.; Zhao, Y.; Yu, Y.; Hu, L.; Yao, W. Recent developments of nanoenzyme-based colorimetric sensors for heavy metal detection and the interaction mechanism. *Analyst* **2020**, *145*, 3173–3187. [\[CrossRef\]](#) [\[PubMed\]](#)
24. Tang, Y.; Hu, Y.; Yang, Y.; Liu, B.; Wu, Y. A facile colorimetric sensor for ultrasensitive and selective detection of Lead(II) in environmental and biological samples based on intrinsic peroxidase-mimic activity of WS2 nanosheets. *Anal. Chim. Acta* **2020**, *1106*, 115–125. [\[CrossRef\]](#) [\[PubMed\]](#)
25. Han, K.N.; Choi, J.-S.; Kwon, J. Gold nanozyme-based paper chip for colorimetric detection of mercury ions. *Sci. Rep.* **2017**, *7*, 1–7. [\[CrossRef\]](#)
26. Peng, C.-F.; Zhang, Y.-Y.; Wang, L.-Y.; Jin, Z.-Y.; Shao, G. Colorimetric assay for the simultaneous detection of Hg2+ and Ag+ based on inhibiting the peroxidase-like activity of core-shell Au@Pt nanoparticles. *Anal. Methods* **2017**, *9*, 4363–4370. [\[CrossRef\]](#)
27. Lien, C.-W.; Tseng, Y.-T.; Huang, C.-C.; Chang, H.-T. Logic Control of Enzyme-Like Gold Nanoparticles for Selective Detection of Lead and Mercury Ions. *Anal. Chem.* **2014**, *86*, 2065–2072. [\[CrossRef\]](#)
28. Liu, B.; Liu, J. Surface modification of nanozymes. *Nano Res.* **2017**, *10*, 1125–1148. [\[CrossRef\]](#)
29. Tripathi, R.M.; Park, S.H.; Kim, G.; Kim, D.-H.; Ahn, D.; Kim, Y.M.; Kwon, S.J.; Yoon, S.-Y.; Kang, H.J.; Chung, S.J. Metal-induced redshift of optical spectra of gold nanoparticles: An instant, sensitive, and selective visual detection of lead ions. *Int. Biodeterior. Biodegrad.* **2019**, *144*. [\[CrossRef\]](#)

30. Sun, J.; Lu, Y.; He, L.; Pang, J.; Yang, F.; Liu, Y. Colorimetric sensor array based on gold nanoparticles: Design principles and recent advances. *TrAC Trends Anal. Chem.* **2019**, *122*, 115754. [\[CrossRef\]](#)
31. Onireti, O.O.; Lin, C.; Qin, J. Combined effects of low-molecular-weight organic acids on mobilization of arsenic and lead from multi-contaminated soils. *Chemosphere* **2017**, *170*, 161–168. [\[CrossRef\]](#)
32. Wu, Y.-S.; Huang, F.-F.; Lin, Y.-W. Fluorescent Detection of Lead in Environmental Water and Urine Samples Using Enzyme Mimics of Catechin-Synthesized Au Nanoparticles. *ACS Appl. Mater. Interfaces* **2013**, *5*, 1503–1509. [\[CrossRef\]](#)
33. Yoosaf, K.; Ipe, B.I.; Suresh, C.H.; Thomas, K.G. In Situ Synthesis of Metal Nanoparticles and Selective Naked-Eye Detection of Lead Ions from Aqueous Media. *J. Phys. Chem. C* **2007**, *111*, 12839–12847. [\[CrossRef\]](#)
34. Cruz, B.H.; Díaz-Cruz, J.M.; Ariño, C.; Esteban, M. Heavy Metal Binding by Tannic Acid: A Voltammetric Study. *Electroanalysis* **2000**, *12*, 1130–1137. [\[CrossRef\]](#)
35. Zhan, K.; Li, Z.; Chen, J.; Hou, Y.; Zhang, J.; Sun, R.; Bu, Z.; Wang, L.; Wang, M.; Chen, X.; et al. Tannic acid modified single nanopore with multivalent metal ions recognition and ultra-trace level detection. *Nano Today* **2020**, *33*, 100868. [\[CrossRef\]](#)
36. Jiang, C.; Ma, M.; Wang, Y. Using gallic acid-modified gold nanoassemblies to detect the Pb²⁺ of tea. *Anal. Methods* **2012**, *4*, 3570–3574. [\[CrossRef\]](#)
37. Long, Y.J.; Li, Y.F.; Liu, Y.; Zheng, J.J.; Tang, J.; Huang, C.Z. Visual observation of the mercury-stimulated peroxidase mimetic activity of gold nanoparticles. *Chem. Commun.* **2011**, *47*, 11939–11941. [\[CrossRef\]](#) [\[PubMed\]](#)
38. Ma, X.; Chen, Z.; Kannan, P.; Lin, Z.; Qiu, B.; Guo, L. Gold Nanorods as Colorful Chromogenic Substrates for Semiquantitative Detection of Nucleic Acids, Proteins, and Small Molecules with the Naked Eye. *Anal. Chem.* **2016**, *88*, 3227–3234. [\[CrossRef\]](#) [\[PubMed\]](#)
39. Held, K.D.; Sylvester, F.C.; Hopcia, K.L.; Biaglow, J.E. Role of Fenton Chemistry in Thiol-Induced Toxicity and Apoptosis. *Radiat. Res.* **1996**, *145*, 542–553. [\[CrossRef\]](#)
40. Jiang, D.; Ni, D.; Rosenkrans, Z.T.; Huang, P.; Yan, X.; Cai, W. Nanozyme: New horizons for responsive biomedical applications. *Chem. Soc. Rev.* **2019**, *48*, 3683–3704. [\[CrossRef\]](#) [\[PubMed\]](#)
41. Jiang, B.; Duan, D.; Gao, L.; Zhou, M.; Fan, K.; Tang, Y.; Xi, J.; Bi, Y.; Tong, Z.; Gao, G.F.; et al. Standardized assays for determining the catalytic activity and kinetics of peroxidase-like nanozymes. *Nat. Protoc.* **2018**, *13*, 1506–1520. [\[CrossRef\]](#) [\[PubMed\]](#)
42. Fan, K.; Wang, H.; Xi, J.; Liu, Q.; Meng, X.; Duan, D.; Gao, L.; Yan, X. Optimization of Fe₃O₄ nanozyme activity via single amino acid modification mimicking an enzyme active site. *Chem. Commun.* **2017**, *53*, 424–427. [\[CrossRef\]](#)
43. Josephy, P.D.; Eling, T.; Mason, R.P. The horseradish peroxidase-catalyzed oxidation of 3,5,3',5'-tetramethylbenzidine. Free radical and charge-transfer complex intermediates. *J. Biol. Chem.* **1982**, *257*, 3669–3675. [\[CrossRef\]](#)
44. Noh, K.-C.; Nam, Y.-S.; Lee, H.-J.; Lee, K.-B. A colorimetric probe to determine Pb²⁺ using functionalized silver nanoparticles. *Anal.* **2015**, *140*, 8209–8216. [\[CrossRef\]](#)
45. Chen, P.; Zhang, R.; Jiang, Q.; Xiong, X.; Deng, S. Colorimetric Detection of Lead Ion Based on Gold Nanoparticles and Lead-Stabilized G-Quartet Formation. *J. Biomed. Sci. Eng.* **2015**, *08*, 7. [\[CrossRef\]](#)
46. Priyadarshini, E.; Pradhan, N. Metal-induced aggregation of valine capped gold nanoparticles: An efficient and rapid approach for colorimetric detection of Pb²⁺ ions. *Sci. Rep.* **2017**, *7*, 9278. [\[CrossRef\]](#) [\[PubMed\]](#)
47. Xie, Z.-J.; Shi, M.-R.; Wang, L.-Y.; Peng, C.-F.; Wei, X.-L. Colorimetric determination of Pb²⁺ ions based on surface leaching of Au@Pt nanoparticles as peroxidase mimic. *Microchim. Acta* **2020**, *187*, 255. [\[CrossRef\]](#)
48. Zhang, Y.; Leng, Y.; Miao, L.; Xin, J.; Wu, A. The colorimetric detection of Pb²⁺ by using sodium thiosulfate and hexadecyl trimethyl ammonium bromide modified gold nanoparticles. *Dalton Trans.* **2013**, *42*, 5485–5490. [\[CrossRef\]](#)
49. Okoli, B.J.; Shilowa, P.M.; Anyanwu, G.O.; Modise, J.S. Removal of Pb²⁺ from Water by Synthesized Tannin Resins from Invasive South African Trees. *Water* **2018**, *10*, 648. [\[CrossRef\]](#)
50. Zou, L.; Shao, P.; Zhang, K.; Yang, L.; You, D.; Shi, H.; Pavlostathis, S.G.; Lai, W.; Liang, D.; Luo, X. Tannic acid-based adsorbent with superior selectivity for lead(II) capture: Adsorption site and selective mechanism. *Chem. Eng. J.* **2019**, *364*, 160–166. [\[CrossRef\]](#)